Available online at www.sciencedirect.com

ScienceDirect

www.elsevier.com/locate/jes

JES JOURNAL OF ENVIRONMENTAL SCIENCES www.jesc.ac.cn

Changes in visibility with $PM_{2.5}$ composition and relative humidity at a background site in the Pearl River Delta region

Xiaoxin Fu[1,2], Xinming Wang[1,3,], Qihou Hu[1], Guanghui Li[1,2], Xiang Ding[1], Yanli Zhang[1], Quanfu He[1,2], Tengyu Liu[1,2], Zhou Zhang[1,2], Qingqing Yu[1,2], Ruqing Shen[1,2], Xinhui Bi[1]*

1. *State Key Laboratory of Organic Geochemistry, Guangzhou Institute of Geochemistry, Chinese Academy of Sciences, Guangzhou 510640, China*
2. *University of Chinese Academy of Sciences, Beijing 100049, China*
3. *Guangdong Key Laboratory of Environmental Resources Utilization and Protection, Guangzhou Institute of Geochemistry, Chinese Academy of Sciences, Guangzhou 510640, China*

ARTICLE INFO

Article history:
Received 31 May 2015
Revised 8 August 2015
Accepted 18 August 2015
Available online 17 December 2015

Keywords:
$PM_{2.5}$
Visibility
Mass scattering efficiency
Light extinction coefficient
Relative humidity

ABSTRACT

In fall–winter, 2007–2013, visibility and light scattering coefficients (b_{sp}) were measured along with $PM_{2.5}$ mass concentrations and chemical compositions at a background site in the Pearl River Delta (PRD) region. The daily average visibility increased significantly ($p < 0.01$) at a rate of 1.1 km/year, yet its median stabilized at ~13 km. No haze days occurred when the 24-hr mean $PM_{2.5}$ mass concentration was below 75 μg/m^3. By multiple linear regression on the chemical budget of particle scattering coefficient (b_{sp}), we obtained site-specific mass scattering efficiency (MSE) values of 6.5 ± 0.2, 2.6 ± 0.3, 2.4 ± 0.7 and 7.3 ± 1.2 m^2/g, respectively, for organic matter (OM), ammonium sulfate (AS), ammonium nitrate (AN) and sea salt (SS). The reconstructed light extinction coefficient (b_{ext}) based on the Interagency Monitoring of Protected Visual Environments (IMPROVE) algorithm with our site-specific MSE revealed that OM, AS, AN, SS and light-absorbing carbon (LAC) on average contributed 45.9% ± 1.6%, 25.6% ± 1.2%, 12.0% ± 0.7%, 11.2% ± 0.9% and 5.4% ± 0.3% to light extinction, respectively. Averaged b_{ext} displayed a significant reduction rate of 14.1/Mm·year ($p < 0.05$); this rate would be 82% higher if it were not counteracted by increasing relative humidity (RH) and hygroscopic growth factor (f(RH)) at rates of 2.5% and 0.16/year^{-1} ($p < 0.01$), respectively, during the fall–winter, 2007–2013. This growth of RH and f(RH) partly offsets the positive effects of lowered AS in improving visibility, and aggravated the negative effects of increasing AN to impair visibility.

Introduction

High $PM_{2.5}$ (particulate matters with aerodynamic diameters less than 2.5 μm) mass loading and its impacts on public health and visibility have become China's most pressing air quality problem in recent years (Chang et al., 2009; Chen et al., 2012b; Zhang et al., 2012a). As the deteriorated visibility is mainly due to visible light extinction by fine particles, the light extinction coefficient (b_{ext}) is a vital parameter to reveal ambient air pollution by $PM_{2.5}$ (Malm et al., 1994; Watson, 2002). Theoretically, b_{ext} is affected by the nature of airborne particles, such as size distribution, chemical composition,

* *Corresponding author.*
E-mail address: wangxm@gig.ac.cn (X. Wang).

http://dx.doi.org/10.1016/j.jes.2015.12.001
1001-0742/

mixing state and hygroscopic behavior (Seinfeld and Pandis, 2006). Due to the costly instruments and intractable database involved, most routine field sampling has not involved measuring particle sizes, mixing state and hygroscopicity. Hence, calculating b_{ext} based on classical Mie theory could not be widely adopted at ordinary monitoring sites. Alternatively, the project of Interagency Monitoring of Protected Visual Environments (IMPROVE) in the United States provides a prompt and practical method to reconstruct b_{ext} (IMPROVE Report V, 2011).

The IMPROVE algorithm is a concise way to link b_{ext} with the major chemical components of particles, and therefore has been broadly used in previous studies to reconstruct the chemical budget of b_{ext} (Hand and Malm, 2006; Malm and Hand, 2007; Yang et al., 2007; Jung et al., 2009; Cao et al., 2012; Lin et al., 2014; Tao et al., 2014a, 2014b). However, the mass scattering/absorbing efficiency (MSE/MAE) and hygroscopic growth factor (f(RH)) set in the IMPROVE algorithm is only an approximation and simplification, and its extensive use in other sites, particularly ones in heavily polluted area, is always under question. MSE, for instance, has usually showed a large discrepancy from site to site. As in the United States, the MSE for dry AS ranged from 1.5 m^2/g in Big Bend National Park to 4.3 m^2/g in southern New Hampshire. MSE for OM was 0.9 m^2/g in the Mount Zirkel Wilderness Area and 4.1 m^2/g in Glacier National Park (Watson et al., 2001; Hering et al., 2003; Hand and Malm, 2007; Malm and Hand, 2007). Hence, the MSE values derived from measurements in the US national parks in the IMPROVE method might not suit other sites in the world. Considering this, many researchers attempted to obtain site-specific MSE instead (Jung et al., 2009; Cheng et al., 2014; Tao et al., 2014a, 2014b). On the other hand, although sulfate (SO_4^{2-}), nitrate (NO_3^-), ammonium (NH_4^+) and organic matter (OM) constituted approximately 80% of the mass concentration of $PM_{2.5}$ (Yang et al., 2011; Fu et al., 2014), they are found to vary in their influence on optical and hygroscopic properties (Stock et al., 2011; Chen et al., 2012a; Tan et al., 2013). $(NH_4)_2SO_4$ (AS) and NH_4NO_3 (AN) are recognized as major components governing the hygroscopic growth of aerosols and by contrast, the hygroscopicity of OM is negligible (Malm et al., 2003; Aggarwal et al., 2007; Wang et al., 2014a). As a consequence, while the change of b_{ext} with OM is largely linear, the influence on b_{ext} by AS and AN in essence is the combined effect of the mass concentration and hygroscopic growth. In this situation, if one wants to relate the change of visibility or b_{ext} to that of particle compositions, relative humidity (RH) is a factor that cannot be ignored.

The Pearl River Delta (PRD) region is one of China's most densely populated and economically developed city clusters. Due to the effective pollution control in the last decade, the annual number of days with haze, which refers to occurrence of visibility <10 km at RH < 90%, has decreased from the maximum of over 200 days during the 1990s to ~50 days in last several years. As observed at a background site in Guangzhou during fall–winter, the seasons when haze days are much more frequent, the observed average mass concentration of $PM_{2.5}$ decreased significantly from 112.5 $\mu g/m^3$ in 2007 to 78.6 $\mu g/m^3$ in 2011, with a rate of −8.6 $\mu g/(m^3 \cdot year)$, and more specifically, while mass concentrations of sulfate and carbonaceous aerosols decreased, that of nitrate has increased during the years (Fu et al., 2014). In this study, we investigated the annual trends of visibility and b_{ext} in the heavily polluted fall–winter seasons during 2007–2013 based on our observations at a background site in the PRD region, and further explored the role of RH and the chemical composition of $PM_{2.5}$ in the changes in visibility.

1. Experimental

1.1. Field Sampling

The PRD region facilitates the accumulation of pollutants under the influence of high-pressure ridges and northeasterly monsoonal winds in fall–winter (Ding and Chan, 2005). Stagnant meteorological conditions and the long-lasting sunny days in these seasons lead to severe air pollution in the PRD region (Fan et al., 2008). In this study, the field campaigns were conducted in the most polluted fall–winter seasons each year on the rooftop of a 5-storey building in the campus of a middle school at Wanqingsha (WQS; 22.42°N, 113.32°E), a town located in rural Guangzhou and also in the center of the PRD (Fig. 1). Since the surrounding areas have low traffic flow and few factories, the local anthropogenic emissions are not significant at this rural site. Hence, this site is an ideal one to study regional air pollution and is included in the regional air quality monitoring network in the PRD region.

Twenty four-hr $PM_{2.5}$ samples were collected by drawing air through 8 inch × 10 inch quartz filters (QMA, Whatman, UK) using a high-volume sampler ($HVPM_{2.5}$, Tisch Environmental Inc., USA) at a rate of 1.1 ± 0.04 m^3/min (average ± 95% confidence interval, the same as follows). The quartz filters were pre-baked at 450°C for 4 hr prior to field sampling and stored at −20°C after sampling until analysis. Thirty two, twenty nine, twenty five, fifty three, twenty six, forty one and twenty nine $PM_{2.5}$ filter samples were collected in 2007, 2008, 2009, 2010, 2011, 2012 and 2013, respectively. Details of the meteorology during the sampling periods and the site were reported previously (Fu et al., 2014, 2015). During the sampling periods, blank $PM_{2.5}$ samples were collected every week.

Fig. 1 – Sampling site at Wanqingsha (WQS) and the surrounding environment.

During fall–winter of 2011–2013, a three-wavelength integrating Nephelometer (Aurora-3000, Ecotech Pty Ltd., Australia) was used to measure the light scattering coefficient (for light scattering angles between 10 ° and 170°) of dry aerosol (RH < 40% ± 2%) at wavelengths of 450, 525 and 635 nm. No size-selective inlets were used. The nephelometer was operated at 5 L/min and data resolution was 1 min. The data for wavelength of 525 nm was chosen for discussion in this study. The data were corrected for truncation errors and the non-Lambertian light source following the widely used method (Anderson and Ogren, 1998) where a linear function of the Angstrom exponent $å_{450/635}$ was used. We estimated a total nephelometer correction factor of 1.15 ± 0.02 for this study.

Visibility was detected using a Belfort Model 6000 visibility sensor (Model 6000, Belfort Instrument, USA). The meteorological parameters including wind speed/direction, temperature and RH were measured by a mini weather station (Vantage Pro2™, Davis Instruments Corp., USA). All the measured 1-min resolution data for light scattering coefficient, visibility, RH and temperature were averaged to 24-hr data according to the precise $PM_{2.5}$-sampling hours.

1.2. Chemical Analysis

The detailed procedure for chemical analysis procedure was given in Fu et al. (2014). In brief, after 24-hr equilibration at temperature 20–25°C and RH 35%–45%, $PM_{2.5}$ filters were weighed twice before and after field sampling to obtain filter-based mass concentrations of $PM_{2.5}$.

For analysis of water-soluble inorganic ions, a punch (5.06 cm^2) of the filters was extracted twice with 10 mL ultrapure Milli-Q water for 15 min each using an ultrasonic ice-water bath. The 20 mL water extracts were then filtered through a 0.22 μm pore size polytetrafluoroethylene (PTFE)-filter and stored in a high-density polyethylene (HDPE) bottle. The cations (Na^+, NH_4^+, K^+, Mg^{2+} and Ca^{2+}) and anions (Cl^-, NO_3^-, and SO_4^{2-}) were analyzed with an ion-chromatography (883 Basic IC plus, Metrohm, Switzerland). The organic carbon (OC) and elemental carbon (EC) in $PM_{2.5}$ were determined using an OC/EC analyzer (OC/EC carbon aerosol analyzer, Sunset Laboratory Inc., USA) (NIOSH, 1999).

1.3. Quality Assurance/Quality Control (QA/QC)

During the sampling periods, the flow rate of the $PM_{2.5}$ sampler was calibrated monthly by using a manometer (S/N 9323995, Thermo, USA) to measure the pressure differential across the filter. The field and laboratory blank samples were analyzed in the same way as field samples. All the OC/EC and cation/anion data were corrected using the field blanks. The average concentrations of blank samples in water extracts for Na^+, NH_4^+, K^+, Mg^{2+}, Ca^{2+}, Cl^-, NO_3^- and SO_4^{2-} were 0.03 ± 0.01, 0.00 ± 0.01, 0.02 ± 0.01, 0.02 ± 0.01 0.02 ± 0.01, 0.03 ± 0.01, 0.05 ± 0.02, 0.04 ± 0.02 ppm, respectively, while the average values of OC and EC in the blank filter were 0.29 ± 0.22, 0.00 ± 0.21 μg C/cm^2, respectively. The method detection limits (MDLs) were 0.05, 0.01–0.05, and 0.02–0.03 μg/m^3 for OC/EC, cations, and anions, respectively.

For the Nephelometer, zero calibration was performed every day with particle-free air to subtract the Rayleigh-scattering component from the b_{ext}. The daily drifts of the zero point were <1.0/Mm. Span calibrations were performed weekly using particle free HFC-R134a gas (99.99% purity).

2. Results and Discussion

2.1. Visibility and $PM_{2.5}$ Mass Concentrations

The trend of daily average visibility in fall–winter of 2007–2013 is shown in Fig. 2a. The annual average visibilities significantly increased from 11.7 ± 1.1 km in 2007 to 22.2 ± 3.9 in 2013 (*F*-test, $p < 0.01$), with a rate of 1.1 km/year. However, the median visibilities in these years stabilized at 13.4 ± 2.5 km (*F*-test, $p = 0.2$). If the visibilities were further divided into two groups according to the threshold of daily average visibility of 14 km for all the field campaigns in this study, the visibilities above 14 km displayed a significant growth trend at a rate of 3.4 km/year (*F*-test, $p < 0.01$), while the visibilities below 14 km did not show obvious improvement (*F*-test, $p = 0.9$). Furthermore, the mean visibilities of the best 20% and worst 20% observed in this study were 25.9 ± 2.1 and 7.0 ± 0.4 km (Fig. 2b), respectively; compared to values of 14 and 7 km, respectively, observed in summer 2006 in Guangzhou (Jung et

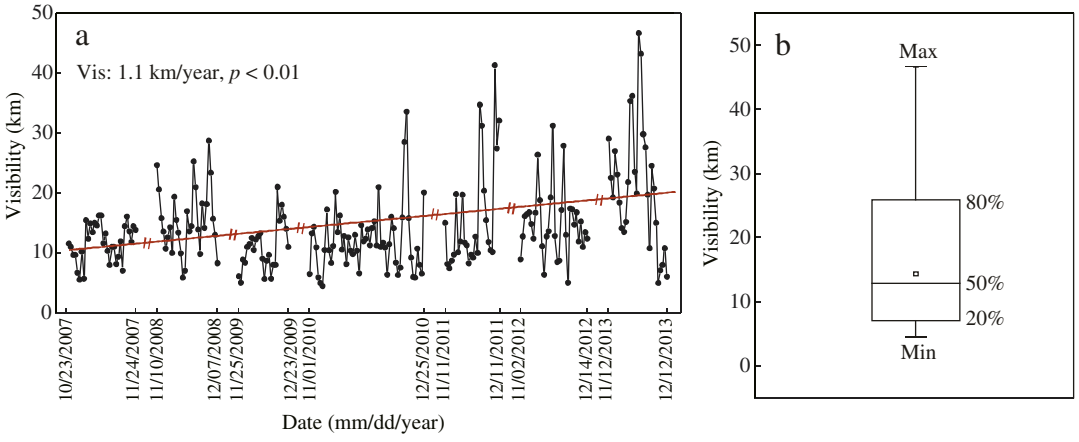

Fig. 2 – (a) Annual variation of 24-hr visibility (vis) and (b) box plot of 24-hr visibility in fall and winter of 2007–2013.

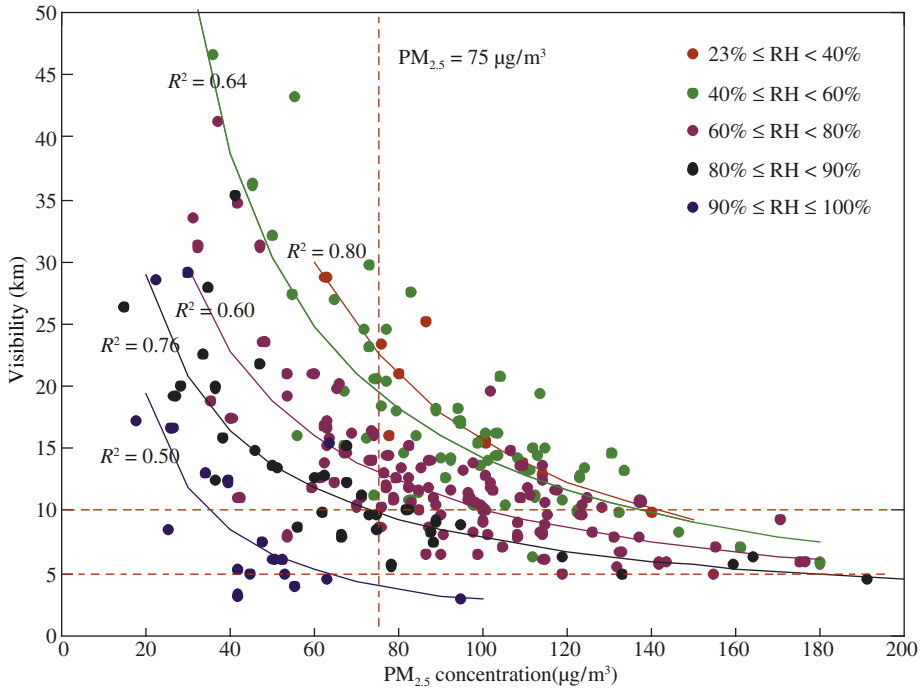

Fig. 3 – Visibility as a power function of $PM_{2.5}$ mass in fall and winter of 2007–2013. Data points are colored to represent different relative humidity (RH).

al., 2009), the visibility of the best 20% seemed to increase substantially. This improvement may be largely attributed to the decrease of $PM_{2.5}$ and its major components (sulfate and OM) with the tightening of emission control in the PRD region (Fu et al., 2014).

As shown in Fig. 3, the visibility decreased with the increasing mass concentrations of $PM_{2.5}$ by a power function in different RH ranges during the fall–winter of 2007–2013. During our campaigns, visibility on 28 November 2013 maximized at 47 km with RH of 40%–60% and $PM_{2.5}$ concentration of 35.8 μg/m^3, the lowest of all samples. Contrarily, on 6 November 2010 the visibility was only 4 km when $PM_{2.5}$ soared to 191.1 μg/m^3 under RH 87%. Among all our 225 sampling days during fall–winter of 2007–2013, 86% (193 days) recorded visibility ≤20 km, 21% (48 days) were haze days, and still 2% (4 days) suffered extremely low visibility (≤5 km), and these 4 days with extremely low visibility all occurred with corresponding $PM_{2.5}$ over 119 μg/m^3. Deng et al. (2008) also observed that the extremely low visibility days in Guangzhou in November, 2005 were related to $PM_{2.5}$ concentrations of 200–250 μg/m^3. It is noteworthy that about 60% of our samples recorded daily mean $PM_{2.5}$ levels beyond the 75 μg/m^3 level set in the National Ambient Air Quality Standard (NAAQS, GB 3095-2012) of China.

As shown in Fig. 3, at the same $PM_{2.5}$ levels, visibility apparently decreased with elevated RH. In dry conditions (23% ≤ RH < 60%), the threshold mass concentration of $PM_{2.5}$ corresponding to the visibility of 10 km was 138 μg/m^3; however, under RH of 80%–90%, this threshold was lowered to 74 μg/m^3, which was near the 24-hr $PM_{2.5}$ standard of 75 μg/m^3 in the newly-released NAAQS (GB 3095-2012), suggesting that this limit of 75 μg/m^3 for $PM_{2.5}$ could largely prevent the occurrence of hazy days in the PRD region in fall–winter seasons. This $PM_{2.5}$ threshold in Guangzhou was lower than that of ~110 μg/m^3 in Beijing or ~88 μg/m^3 in Xi'an (Zhao et al., 2011; Cao et al., 2012), but higher than that of 42 μg/m^3 in Guangzhou during the 16th Asian Game periods (Tao et al., 2015). This difference might be rooted in the varying meteorological conditions and $PM_{2.5}$ chemical compositions among the field campaigns. In any case, the lower thresholds in Guangzhou than in Beijing or Xi'an means that to guarantee the absence of hazy days, ambient $PM_{2.5}$ should be reduced to much lower levels in Guangzhou, probably due to the higher RH in south China than in the north.

Among the 225 days of our field campaigns, there were only 3 days in which daily average visibility remained lower than 10 km while daily mean $PM_{2.5}$ was below 75 μg/m^3 and RH was below 90%. This abnormality might be due to the light rains during these days. The drizzly weather reduced the mass concentration of $PM_{2.5}$ *via* wet deposition, but at the same time increased local RH and thus deteriorated the visibility (Andronache, 2004). Additionally, there were 10 days with visibility <10 km but RH > 96% with $PM_{2.5}$ ranging 20–60 μg/m^3. As they could not be termed as haze days, the 10 days are not included in the discussion.

2.2. MSE, b_{sp} and b_{ext}

2.2.1. Calculating MSE and Reconstructing the Light Extinction Coefficient (b_{ext})

As soil dust and coarse particles had negligible contribution to aerosol mass and light extinction in the PRD region (Andreae et al., 2008; Wang et al., 2012), only OM, AS, AN, LAC and SS

were involved in this study in calculating b_{ext}. The method of reconstructing the mass of these species in $PM_{2.5}$ followed the IMPROVE algorithm, *i.e.*, AS = 1.375[sulfate], AN = 1.29 [nitrate], LAC = [EC] and SS = 1.8[chloride]. Since the air masses arriving at WQS were relatively aged, the conversion factor for OC to OM was chosen as 2, *i.e.*, OM = 2[OC] (Andreae et al., 2008; Fu et al., 2014, 2015). The reconstructed average mass concentrations of OM, AS, AN, LAC and SS during fall–winter of 2007–2013 were 35.0 ± 2.0, 22.3 ± 1.3, 11.8 ± 1.0, 3.4 ± 0.2 and 2.7 ± 0.3 μg/m^3, respectively. They totally accounted for 86.6% ± 2.1% of the measured $PM_{2.5}$. Since LAC is only responsible for light absorption, multiple linear regression (MLR) could be applied to deduce site specific MSE values with available dataset chemical components and b_{sp} measured under relatively dry conditions by Nephelometer as below:

$$b_{sp} = a_1 \times [OM] + a_2 \times [AS] + a_3 \times [AN] + a_4 \times [SS] \quad (1)$$

where a_1, a_2, a_3 and a_4 are MSEs, which were revealed from the MLR ($R^2 = 0.94$, $p < 0.01$) to be 6.5 ± 0.2, 2.6 ± 0.3, 2.4 ± 0.7 and 7.3 ± 1.2 m^2/g, respectively, for OM, AS, AN and SS. If we adopted MAE of 7.7 m^2/g for LAC obtained by Andreae et al. (2008) in Guangzhou during fall–winter, b_{ext} could then be estimated as:

$$b_{ext} = 6.5 \times [OM] + 2.6 \times f(RH) \times [AS] + 2.4 \times f(RH) \times [AN] + 7.3 \times f(RH)_{ss} \times [SS] + 7.7 \times [LAC]. \quad (2)$$

The hygroscopic growth factor f(RH) for AS and AN, and $f(RH)_{ss}$ for SS were obtained from the tabulated values in Malm et al. (1994) and Pitchford et al. (2007), respectively. Rayleigh scattering (~10/Mm) was negligible and hence not included in the equation (IMPROVE Report V, 2011).

MSE for OM in this study was comparable with those previously reported in fall–winter in China, for example 6.2 m^2/g in Guangzhou (Tao et al., 2014b) and 6.3 m^2/g in Shanghai (Cheng et al., 2014), but higher than these previously reported in the summer, such as 4.9 m^2/g in Guangzhou (Jung et al., 2009) and 4.2 m^2/g in the Mediterranean (Sciare et al., 2005), and twice as high as the average of 3.1 m^2/g derived by MLR in the review by Hand and Malm (2007). Our MSE values for AS and AN were comparable with those of 2.8 m^2/g by Hand and Malm (2007) and 2.4 m^2/g by Jung et al. (2009), but much lower than those of 3.5 m^2/g for AS and 4.3 m^2/g for AN by Cheng et al. (2014), and 5.3 m^2/g for AS and 5.5 m^2/g for AN by Tao et al. (2014b). This discrepancy in MSE might have partly resulted from the algorithms used, *i.e.* MRL *versus* theoretical calculation. Nonetheless, site specific properties, size distribution and chemical composition of aerosols are vital factors behind this discrepancy. It is worth noting that taking all chloride as SS-related will overestimate SS, since short-lived chlorinated hydrocarbons were present, which were widely used in China's highly industrialized PRD region (Zhang et al., 2012b), and their degradation in the ambient will also be a source of chloride detected in this study.

During the fall–winters of 2011–2013, b_{sp} for dry aerosols ranged from 71.9 to 571.5/Mm, with an average of 253.2 ± 26.0/Mm. The average was lower than that of 418/Mm measured in winter 2004 in Guangzhou (Andreae et al., 2008), and also lower than that of 473/Mm observed at an urban site in Guangzhou during fall 2009 (Tao et al., 2014b), probably due to a large amount of ultrafine/fine particle from vehicles in the urban areas (Wehner et al., 2002; Dai et al., 2015; Zhang et al., 2015). Average b_{sp} values also were revealed to be relatively higher in China's densely populated city clusters, such as 312/Mm over a rural area near the Beijing mega-city in 2006 (Pan et al., 2009), 456/Mm during winter 2010 in Shanghai in the Yangtze River Delta region (Xu et al., 2012), and 293/Mm in 2011 in Chengdu, a mega-city in southwest China (Tao et al., 2014a). The calculated b_{ext} showed a linear relationship with the measured b_{sp} for dry aerosols (Fig. 4a) with a slope of 0.79, which was in fact the single scattering albedo. This value is quite near that of 0.83 reported previously in Guangzhou (Andreae et al., 2008) or 0.82 in Chengdu (Tao et al., 2014a). A value as low as 0.71 was observed in an urban site of Spain in 2006–2007 (Titos et al., 2012), but it could reach as high as 0.96 in coastal areas of the United States (Magi et al., 2005), and

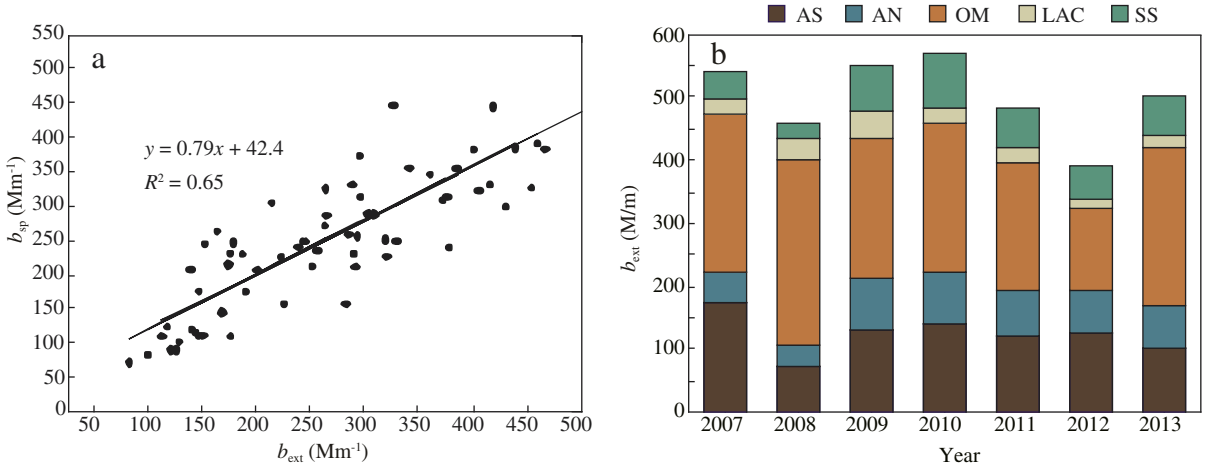

Fig. 4 – (a) Reconstructed light extinction coefficient (b_{ext}) *versus* measured light scattering coefficient (b_{sp}), in dry conditions and (b) chemical budget of b_{ext} in fall and winter of 2007–2013. AS: ammonium sulfate; AN: ammonium nitrate; OM: organic matter; LAC: light-absorbing carbon; SS: sea salt.

Table 1 – Chemical budget of light extinction coefficient (b_{ext}), light extinction by OM, AS, AN, SS and LAC, the reconstructed concentrations (dry) of $PM_{2.5}$ ($PM_{2.5}$) and RH in fall–winter of 2007–2013.

Year	AS (/Mm)	AN (/Mm)	OM (/Mm)	LAC (/Mm)	SS (/Mm)	b_{ext} (/Mm)	$PM_{2.5}$ (μg/m^3)	RH (%)
2007	174.5 ± 24.1	46.5 ± 9.4	250.1 ± 21.6	27.3 ± 2.9	41.6 ± 8.5	540.1 ± 40.5	84 ± 6	68 ± 3
2008	71.8 ± 12.1	35.1 ± 7.7	294.0 ± 37.9	32.6 ± 3.0	27.3 ± 9.9	460.7 ± 60.3	85 ± 10	44 ± 4
2009	130.7 ± 22.0	82.6 ± 18.6	222.7 ± 36.4	42.2 ± 7.0	71.4 ± 20.1	549.5 ± 81.2	81 ± 11	67 ± 5
2010	139.5 ± 21.0	82.2 ± 20.0	236.6 ± 26.9	25.6 ± 3.0	86.0 ± 24.6	569.8 ± 79.4	81 ± 9	71 ± 3
2011	120.8 ± 20.3	74.4 ± 15.3	200.0 ± 28.3	23.9 ± 3.1	63.6 ± 16.8	482.5 ± 67.5	68 ± 8	71 ± 4
2012	127.6 ± 13.2	63.7 ± 19.9	132.8 ± 20.3	13.8 ± 1.1	51.7 ± 13.0	389.5 ± 49.3	48 ± 7	81 ± 3
2013	103.8 ± 29.2	64.8 ± 23.3	251.8 ± 41.4	20.0 ± 2.3	62.3 ± 17.8	502.8 ± 94.4	76 ± 15	67 ± 5
Avg.	126.5 ± 8.9	65.4 ± 7.2	227.3 ± 13.0	26.0 ± 1.6	60.1 ± 7.7	505.2 ± 28.6	75 ± 4	67 ± 9

AS: ammonium sulfate; AN: ammonium nitrate; OM: organic matter; LAC: light-absorbing carbon; SS: sea salt; RH: relative humidity; Avg.: average.
Average ± 95% confidence interval.

0.91 in coastal areas of Norway (Mogo et al., 2012). The lower single scattering albedo in China indicated a larger fraction of absorbing materials in the aerosols.

2.2.2. Chemical Budget of Light Extinction

Based on Eq. (2), the chemical budgets of b_{ext} are listed in Table 1 and illustrated in Fig. 4b. On average, the light extinction by OM, AS, AN, SS and LAC during fall–winter of 2007–2013 was 227.3% ± 13, 126.5% ± 8.9, 65.4% ± 7.2, 60.1% ± 7.7 and 26.0% ± 1.6/Mm, and accounted for 45.9% ± 1.6%, 25.6% ± 1.2%, 12.0% ± 0.7%, 11.2% ± 0.9% and 5.4% ± 0.3% of the total light extinction, respectively. Yu et al. (2010) found that non-EC coating materials contributed 90%–96% of the light extinction at a rural site of the PRD region, consistent with ~95% in our study. OM accounted for the largest proportion of light extinction, comparable with the sum of AS, AN and SS. This dominant contribution of OM to light extinction was also reported in Beijing (57.4%) by Wang et al. (2014b) and in the Indo-Gangetic plain (46%) by Tiwari et al. (2014). However, Jung et al. (2009) reported that AS was the largest contributor to light extinction during summer in Guangzhou; AS was also a dominant contributor in other large cities in China, like Xi'an (39.8%; Cao et al., 2012) and Nanjing (37%; Shen et al., 2014). As shown in Fig. 4b, it was found that the reconstructed annual average b_{ext} was the lowest (389.5/Mm) in 2012, followed by 460.7/Mm in 2008, while the average reconstructed $PM_{2.5}$ concentration (dry) was the highest (85 μg/m^3) in 2008 and the lowest (48 μg/m^3) in 2012. The above results might be caused by the difference in RH, *i.e.*, the average f(RH) in 2012 (3.4) was far higher than in 2008 (1.3).

2.3. Annual Trend of Light Extinction Coefficient (b_{ext})

As shown in Fig. 5, reconstructed b_{ext} ranged from 161.8 to 1617.8/Mm, with an average of 505.2 ± 28.6/Mm. During 2007–2013, fall–winter b_{ext} declined at a rate of 14.1/Mm/year (F-test, $p < 0.05$), which was consistent with the increasing trend of visibility. The average of reconstructed b_{ext} was less than

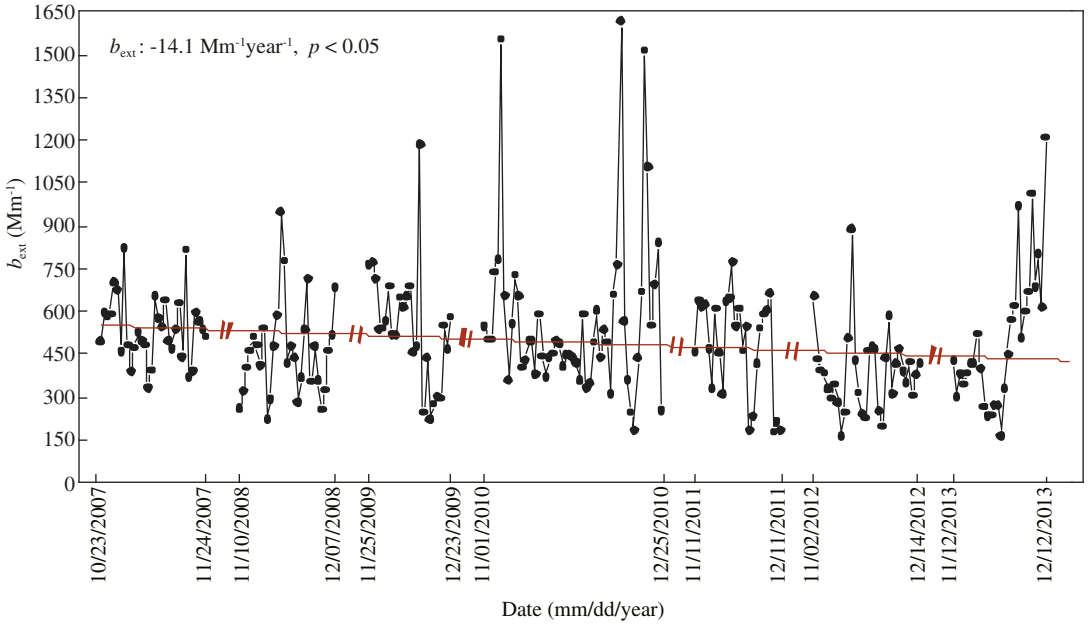

Fig. 5 – Annual variation of 24-hr reconstructed light extinction coefficient (b_{ext}) in fall and winter of 2007–2013.

those reported in winter in Xi'an, China (1328/Mm), in Delhi, India (823/Mm), and in Chengdu, China (708/Mm) (Cao et al., 2012; Tao et al., 2014a; Tiwari et al., 2014). However, b_{ext} in this study was 1.2–3.7 times that reported in summer in Guangzhou, China (419/Mm), in Nanjing, China (249/Mm), and in Atlanta, United States (137/Mm) (Carrico et al., 2003; Jung et al., 2009; Shen et al., 2014).

As discussed in Section 2.1, the annual median visibility seemed to improve less with the significant drop of $PM_{2.5}$ mass concentrations in recent years. According to Eq. (2), b_{ext} from OM and LAC was not affected by RH. Therefore, b_{ext} from OM and LAC would decrease accordingly with the decreasing concentrations of OC and EC (Fu et al., 2014). However, b_{ext} by AS, AN and SS was complicated by RH with f(RH). The trends of AS *vs.* f(RH) × AS and AN *vs.* f(RH) × AN are shown in Fig. 6a and b, respectively. In Fig. 6a, both AS and f(RH) × AS showed a reducing rate of ~1.9 μg/(m^3·year), if f(RH) remained constant, f(RH) × AS would drop more than AS, and changing RH partly counteracted the reduction trend of AS. By contrast, AN showed a slightly increasing trend over the period (p = 0.5; Fig. 6b), and f(RH) × AN had a significant growth of 1.6 μg/(m^3·year) (p < 0.05), indicating that b_{ext} by AN increased during the period. As illustrated in Fig. 7, RH and f(RH) (dimensionless) showed significant (p < 0.01) increases of 2.5% and 0.16/year, respectively. With the time series of monthly average RH from the HadISDH (Met Office Hadley Centre, UK; http://www.metoffice.gov.uk/hadobs/hadisdh/), for the grid box of Guangzhou in fall–winter of 2007–2013, RH recorded an annual growth of 1.1%/year^{-1}. The broad range of the grid box (5° × 5°) and the adjustment process for climatological homogeneity might lead to the difference seen in the increasing trends. Song et al. (2012) found RH increased in south China during 2007–2010, and Lu et al. (2014) also reported that the moisture in southeast

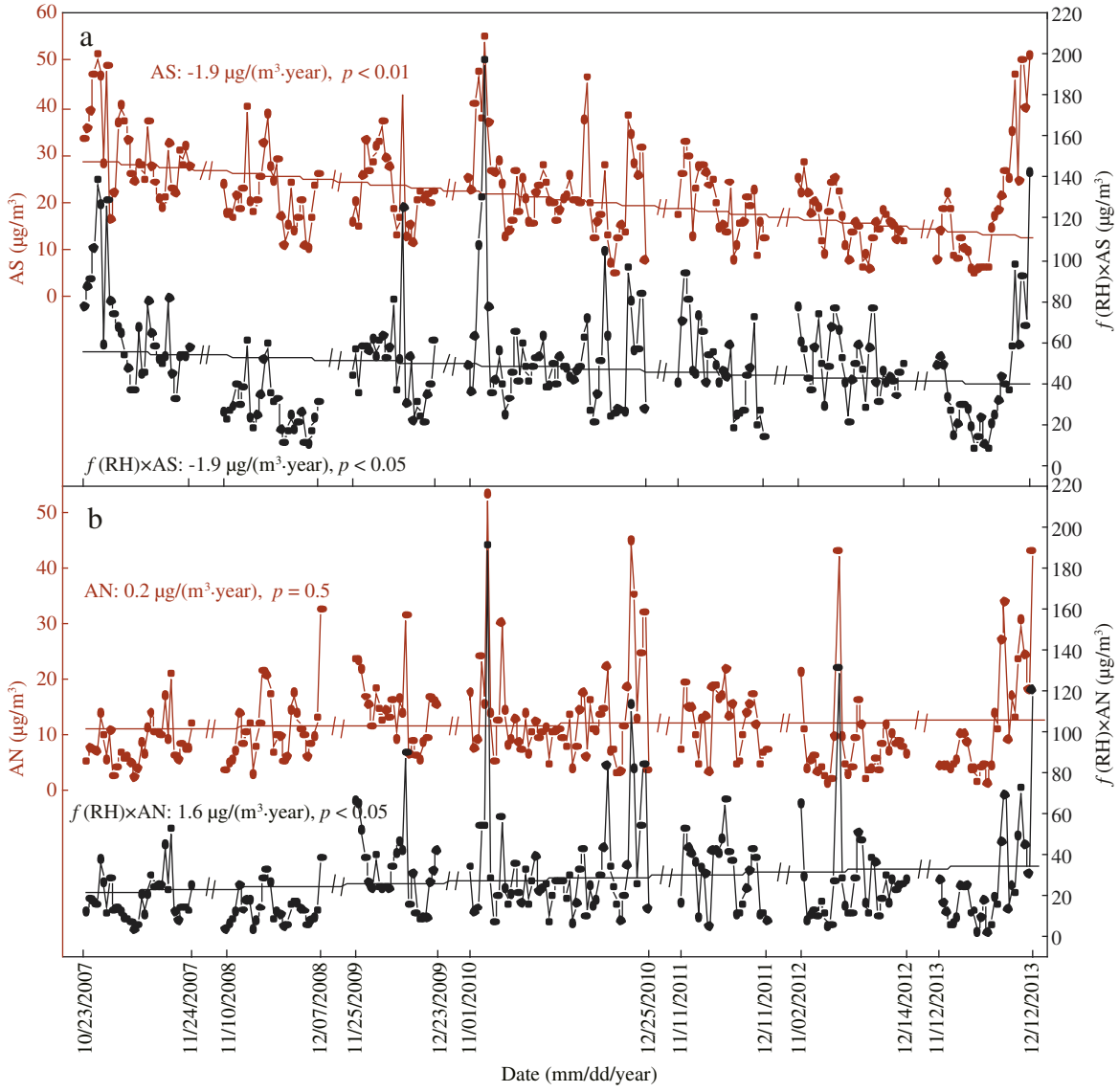

Fig. 6 – Annual variation of (a) reconstructed mass of ammonium sulfate (AS) and hygroscopic growth factor times ammonium sulfate (f(RH) × AS) and (b) reconstructed mass of ammonium nitrate (AN) and hygroscopic growth factor times ammonium nitrate (f(RH) × AN) in fall and winter of 2007–2013.

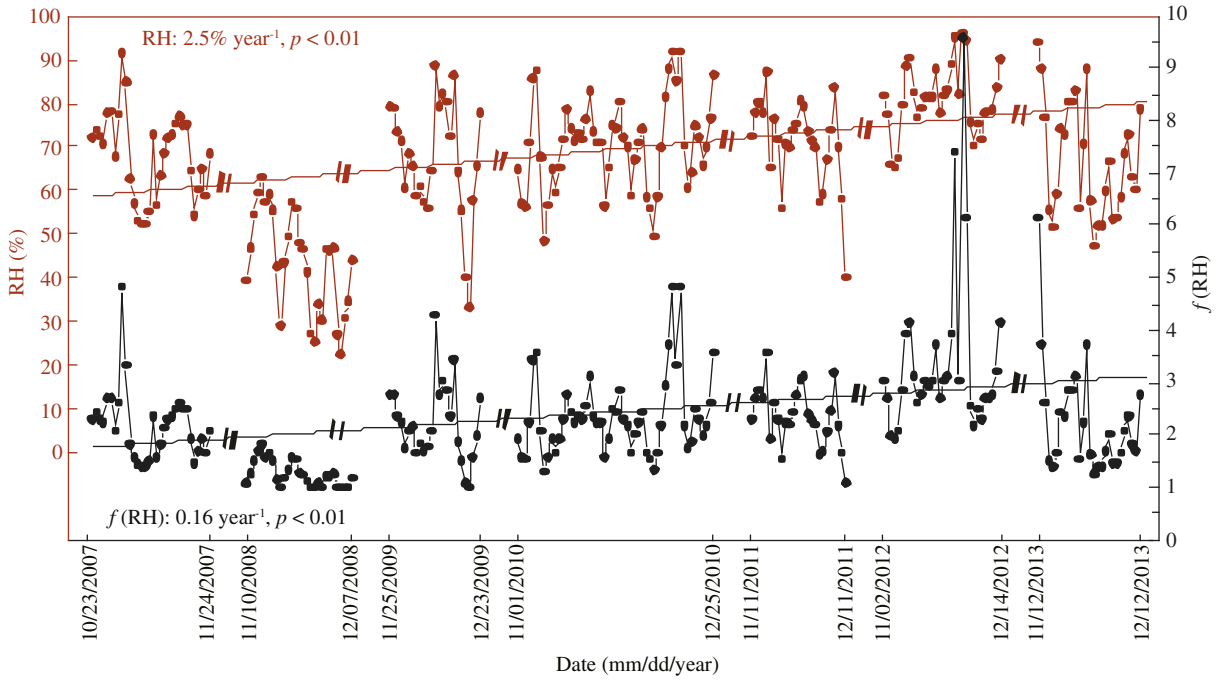

Fig. 7 – Annual variation of 24-hr relative humidity (RH) and hygroscopic growth factor (*f*(RH)) in fall and winter of 2007–2013.

China had an increasing trend in summer. Therefore, the growth of RH and *f*(RH) in recent years weakened the reduction of light extinction by AS, and enhanced the light extinction by increasing AN. Additionally, although SS did not show a clear increasing trend in these years, the co-effect of *f*(RH) and SS also tended to increase the light extinction by SS. If one assumes a constant *f*(RH) and $f(RH)_{ss}$ in these years as their 7-year average, we would obtain a b_{ext} decreasing rate of 25.7/Mm/year ($p < 0.01$), 82% higher than that of 14.1/Mm/year as observed. In general, the unimproved mean of the lowest 20% visibility in fall–winter was partly explained by the increasing trend of RH, which offset the effects of reducing ambient $PM_{2.5}$ mass concentrations by emission control. The average b_{ext} in non-hazy days was 436.1 ± 17.4/Mm. If we take this value as the threshold for the occurrence of haze, and assume that *f*(RH) and $f(RH)_{SS}$ remain constant as the average of all of sampling days, and that in non-haze day concentrations of OM, LAC, AN and SS also stabilized as their averages with light extinction contributions, respectively, of 208, 25, 52 and 53/Mm, sulfate should be limited within 12 μg/m^3 to keep the threshold of 436/Mm. However, sulfate still ranged from 14.2 to 22.7 μg/m^3 in our campaigns, so regional SO_2 emission control needs to be further strengthened (Fu et al., 2014). Nevertheless, the emissions of primary OM, volatile organic compounds (VOCs), nitrogen oxide and ammonia should also be controlled more strictly to improve the visibility in the PRD region.

3. Conclusions

During 2007–2013, we measured $PM_{2.5}$ mass concentrations and chemical compositions along with visibility and light scattering at a background site in the PRD region in fall–winter seasons, when haze days most frequently occurred. We observed a significant increase ($p < 0.01$) of daily average visibility at a rate of 1.1 km/year, yet the median visibility stabilized at ~13 km without significant improvement. It appeared that during the seasons, haze days would not occur when 24-hr mean $PM_{2.5}$ mass concentration was below 75 μg/m^3, the 24-hr limit set in China's NAAQS. MLR between b_{sp} against OM, AS, AN and SS revealed their site-specific MSE values of 6.5 ± 0.2, 2.6 ± 0.3, 2.4 ± 0.7 and 7.3 ± 1.2 m^2/g, respectively. The reconstructed b_{ext} displayed a significant declining rate of 14.1/Mm/year with an average single scattering albedo of 0.79, and OM, AS, AN, SS and LAC on average accounted for 45.9% ± 1.6%, 25.6% ± 1.2%, 12.0% ± 0.7%, 11.2% ± 0.9% and 5.4% ± 0.3% of the reconstructed b_{ext}, respectively. Although for policy-makers, it is convenient to have a chemical budget of b_{ext} to link the visibility improvement with emission control measures for $PM_{2.5}$, the changing visibility is also complicated by the variation of RH. During 2007–2013, the growth of RH and *f*(RH) in fall–winter partly offset the positive effects of reduced AS in improving visibility, and enhanced the negative effects of increasing AN in damaging visibility. If RH had remained constant during the years, b_{ext} would have decreased at a rate 82% higher than observed. As OM and AS are two big contributors to b_{ext}, control of primary OM and particularly volatile organic compounds should be brought to attention while strengthening of SO_2 control in coal-fired power plants is taking effect in the region.

Acknowledgments

This study was funded by Strategic Priority Research Program of the Chinese Academy of Sciences (No. XDB05010200), the Natural Science Foundation of China (Nos. 41025012, 41121063) and the Bureau of Science, Technology and Information of Guangzhou (No. 201300000130).

REFERENCES

Aggarwal, S.G., Mochida, M., Kitamori, Y., Kawamura, K., 2007. Chemical closure study on hygroscopic properties of urban aerosol particles in Sapporo, Japan. Environ. Sci. Technol. 41 (20), 6920–6925.

Anderson, T.L., Ogren, J.A., 1998. Determining aerosol radiative properties using the TSI 3563 integrating nephelometer. Aerosol Sci. Technol. 29 (1), 57–69.

Andreae, M.O., Schmid, O., Yang, H., Chand, D., Yu, J.Z., Zeng, L.M., et al., 2008. Optical properties and chemical composition of the atmospheric aerosol in urban Guangzhou, China. Atmos. Environ. 42 (25), 6335–6350.

Andronache, C., 2004. Estimates of sulfate aerosol wet scavenging coefficient for locations in the Eastern United States. Atmos. Environ. 38 (6), 795–804.

Cao, J.J., Wang, Q.Y., Chow, J.C., Watson, J.G., Tie, X.X., Shen, Z.X., et al., 2012. Impacts of aerosol compositions on visibility impairment in Xi'an, China. Atmos. Environ. 59, 559–566.

Carrico, C.M., Bergin, M.H., Xu, J., Baumann, K., Maring, H., 2003. Urban aerosol radiative properties: measurements during the 1999 Atlanta Supersite Experiment. J. Geophys. Res.-Atmos. 108 (D7), 8422.

Chang, D., Song, Y., Liu, B., 2009. Visibility trends in six megacities in China 1973–2007. Atmos. Res. 94 (2), 161–167.

Chen, J., Zhao, C.S., Ma, N., Liu, P.F., Göbel, T., Hallbauer, E., et al., 2012a. A parameterization of low visibilities for hazy days in the North China Plain. Atmos. Chem. Phys. 12 (11), 4935–4950.

Chen, R.J., Kan, H.D., Chen, B.H., Huang, W., Bai, Z.P., Song, G.X., et al., 2012b. Association of particulate air pollution with daily mortality. Am. J. Epidemiol. 175 (11), 1173–1181.

Cheng, Z., Jiang, J.K., Chen, C.H., Gao, J., Wang, S.X., Watson, J.G., et al., 2014. Estimation of aerosol mass scattering efficiencies under high mass loading: case study for the megacity of Shanghai, China. Environ. Sci. Technol. 49, 831–838.

Dai, S., Bi, X., Chan, L.Y., He, J., Wang, B., Wang, X., et al., 2015. Chemical and stable carbon isotopic composition of $PM_{2.5}$ from on-road vehicle emissions in the PRD region and implications for vehicle emission control policy. Atmos. Chem. Phys. 15, 3097–3108.

Deng, X.J., Tie, X.X., Wu, D., Zhou, X.J., Bi, X.Y., Tan, H.B., et al., 2008. Long-term trend of visibility and its characterizations in the Pearl River Delta (PRD) region,. Atmos. Environ. 42 (7), 1424–1435.

Ding, Y.H., Chan, J.C.L., 2005. The East Asian summer monsoon: an overview. Meteorog. Atmos. Phys. 89 (1), 117–142.

Fan, S.J., Wang, B.M., Tesche, M., Engelmann, R., Althausen, A., Liu, J., et al., 2008. Meteorological conditions and structures of atmospheric boundary layer in October 2004 over Pearl River Delta area. Atmos. Environ. 42 (25), 6174–6186.

Fu, X.X., Wang, X.M., Guo, H., Cheung, K.L., Ding, X., Zhao, X.Y., et al., 2014. Trends of ambient fine particles and major chemical components in the Pearl River Delta region: observation at a regional background site in fall and winter. Sci. Total Environ. 497-498, 274–281.

Fu, X.X., Guo, H., Wang, X.M., Ding, X., He, Q.F., Liu, T.Y., et al., 2015. $PM_{2.5}$ acidity at a background site in the Pearl River Delta region in fall–winter of 2007–2012. J. Hazard. Mater. 286, 484–492.

Hand, J.L., Malm, W.C., 2006. Review of the IMPROVE equation for estimating ambient light extinction coefficients. Cooperative Institute for Research in the Atmosphere. Colorado State University, Colorado, USA.

Hand, J.L., Malm, W.C., 2007. Review of aerosol mass scattering efficiencies from ground-based measurements since 1990. J. Geophys. Res.-Atmos. 112 (D16), D16203.

Hering, S.V., Stolzenburg, M.R., Hand, J.L., Kreidenweis, S.M., Lee, T., Collett, J.L., et al., 2003. Hourly concentrations and light scattering cross sections for fine particle sulfate at Big Bend National Park. Atmos. Environ. 37 (9–10), 1175–1183.

IMPROVE (Interagency Monitoring of Protected Visual Environments) Report V, 2011n. Spatial and seasonal patterns and temporal variability of haze and its constituents in the United States. Cooperative Institute for Research in the Atmosphere. Colorado State University, Colorado, USA.

Jung, J., Lee, H., Kim, Y.J., Liu, X.G., Zhang, Y.H., Gu, J.W., et al., 2009. Aerosol chemistry and the effect of aerosol water content on visibility impairment and radiative forcing in Guangzhou during the 2006 Pearl River Delta campaign. J. Environ. Manag. 90 (11), 3231–3244.

Lin, Y.F., Huang, K., Zhuang, G.S., Fu, J.S., Wang, Q.Z., Liu, T.N., et al., 2014. A multi-year evolution of aerosol chemistry impacting visibility and haze formation over an Eastern Asia megacity, Shanghai. Atmos. Environ. 92, 76–86.

Lu, E., Zeng, Y.T., Luo, Y.L., Ding, Y., Zhao, W., Liu, S.Y., et al., 2014. Changes of summer precipitation in China: the dominance of frequency and intensity and linkage with changes in moisture and air temperature. J. Geophys. Res.-Atmos. 119 (22), 12575–12587.

Magi, B.I., Hobbs, P.V., Kirchstetter, T.W., Novakov, T., Hegg, D.A., Gao, S., et al., 2005. Aerosol properties and chemical apportionment of aerosol optical depth at locations off the US east coast in July and August 2001. J. Atmos. Sci. 62 (4), 919–933.

Malm, W.C., Hand, J.L., 2007. An examination of the physical and optical properties of aerosols collected in the IMPROVE program. Atmos. Environ. 41 (16), 3407–3427.

Malm, W.C., Sisler, J.F., Huffman, D., Eldred, R.A., Cahill, T.A., 1994. Spatial and seasonal trends in particle concentration and optical extinction in the United States. J. Geophys. Res.-Atmos. 99 (D1), 1347–1370.

Malm, W.C., Day, D.E., Kreidenweis, S.M., Collett, J.L., Lee, T., 2003. Humidity-dependent optical properties of fine particles during the Big Bend regional aerosol and visibility observational study. J. Geophys. Res.-Atmos. 108 (D9), 4279.

Mogo, S., Cachorro, V.E., Lopez, J.F., Montilla, E., Torres, B., Rodríguez, E., et al., 2012. In situ measurements of aerosol optical properties and number size distributions in a coastal region of Norway during the summer of 2008. Atmos. Chem. Phys. 12 (13), 5841–5857.

NIOSH, 1999. Method 5040 issue 3 (Interim): elemental carbon (diesel exhaust). NIOSH Manual of Analytical Methods, fourth ed. National Institute of Occupational Safety and Health, Cincinnati, OH.

Pan, X.L., Yan, P., Tang, J., Ma, J.Z., Wang, Z.F., Gbaguidi, A., et al., 2009. Observational study of influence of aerosol hygroscopic growth on scattering coefficient over rural area near Beijing mega-city. Atmos. Chem. Phys. 9 (19), 7519–7530.

Pitchford, M., Malm, W., Schichtel, B., Kumar, N., Lowenthal, D., Hand, J., 2007. Revised algorithm for estimating light extinction from IMPROVE particle speciation data. J. Air Waste Manage. Assoc. 57 (11), 1326–1336.

Sciare, J., Oikonomou, K., Cachier, H., Mihalopoulos, N., Andreae, M.O., Maenhaut, W., et al., 2005. Aerosol mass closure and reconstruction of the light scattering coefficient over the Eastern Mediterranean Sea during the MINOS campaign. Atmos. Chem. Phys. 5 (8), 2253–2265.

Seinfeld, J.H., Pandis, S.M., 2006. Atmospheric Chemistry and Physics: From Air Pollution to Climate Change. second ed. John Wiley and Sons, New York, USA.

Shen, G.F., Xue, M., Yuan, S.Y., Zhang, J., Zhao, Q.Y., Li, B., et al., 2014. Chemical compositions and reconstructed light extinction coefficients of particulate matter in a mega-city. In the western Yangtze River Delta, China. Atmos. Environ. 83, 14–20.

Song, Y.F., Liu, Y.J., Ding, Y.H., 2012. A study of surface humidity changes in China during the recent 50 years. Acta Metall. Sin. 26 (5), 541–553.

Stock, M., Cheng, Y.F., Birmili, W., Massling, A., Wehner, B., Muller, T., et al., 2011. Hygroscopic properties of atmospheric aerosol particles over the Eastern Mediterranean: implications for regional direct radiative forcing under clean and polluted conditions. Atmos. Chem. Phys. 11 (9), 4251–4271.

Tan, H.B., Yin, Y., Gu, X.S., Li, F., Chan, P.W., Xu, H.B., et al., 2013. An observational study of the hygroscopic properties of aerosols over the Pearl River Delta region. Atmos. Environ. 77, 817–826.

Tao, J., Zhang, L.M., Cao, J.J., Hsu, S.C., Xia, X.G., Zhang, Z.S., et al., 2014a. Characterization and source apportionment of aerosol light extinction in Chengdu, southwest China. Atmos. Environ. 95, 552–562.

Tao, J., Zhang, L.M., Ho, K.F., Zhang, R.J., Lin, Z.J., Zhang, Z.S., et al., 2014b. Impact of $PM_{2.5}$ chemical compositions on aerosol light scattering in Guangzhou–the largest megacity in South China. Atmos. Res. 135-136, 48–58.

Tao, J., Zhang, L.M., Zhang, Z.S., Huang, R.J., Wu, Y.F., Zhang, R.J., et al., 2015. Contral of $PM_{2.5}$ in Guangzhou during the 16th Asian Games period: implication for hazy weather prevention. Sci. Total Environ. 508, 57–66.

Titos, G., Foyo-Moreno, I., Lyamani, H., Querol, X., Alastuey, A., Alados-Arboledas, L., 2012. Optical properties and chemical composition of aerosol particles at an urban location: an estimation of the aerosol mass scattering and absorption efficiencies. J. Geophys. Res.-Atmos. 117 (D4), D04206.

Tiwari, S., Srivastava, A.K., Chate, D.M., Safai, P.D., Bisht, D.S., Srivastava, M.K., et al., 2014. Impacts of the high loadings of primary and secondary aerosols on light extinction at Delhi during wintertime. Atmos. Environ. 92, 60–68.

Wang, X.M., Ding, X., Fu, X.X., He, Q.F., Wang, S.Y., Bernard, F., et al., 2012. Aerosol scattering coefficients and major chemical compositions of fine particles observed at a rural site hit the central Pearl River Delta, South China. J. Environ. Sci. 24 (1), 72–77.

Wang, X.M., Ye, X.N., Chen, H., Chen, J.M., Yang, X., Gross, D.S., 2014a. Online hygroscopicity and chemical measurement of urban aerosol in Shanghai, China. Atmos. Environ. 95, 318–326.

Wang, Y.H., Liu, Z.R., Zhang, J.K., Hu, B., Ji, D.S., Yu, Y.C., et al., 2014b. Aerosol physicochemical properties and implication for visibility during an intense haze episode during winter in Beijing. Atmos. Chem. Phys. Discuss. 14 (16), 23375–23413.

Watson, J.G., 2002. Visibility: science and regulation. J. Air Waste Manage. Assoc. 52 (6), 628–713.

Watson, J.G., Chow, J.C., Lowenthal, D.H., Cahill, C.F., Blumenthal, D.L., Richards, L.W., et al., 2001. Aerosol chemical and optical properties during the Mt. Zirkel visibility study. J. Environ. Qual. 30 (4), 1118–1125.

Wehner, B., Birmili, W., Gnauk, T., Wiedensohler, A., 2002. Particle number size distributions in a street canyon and their transformation into the urban-air background: measurements and a simple model study. Atmos. Environ. 36 (13), 2215–2223.

Xu, J.W., Tao, J., Zhang, R.J., Cheng, T.T., Leng, C.P., Chen, J.M., et al., 2012. Measurements of surface aerosol optical properties in winter of Shanghai. Atmos. Res. 109-110, 25–35.

Yang, L.X., Wang, D.C., Cheng, S.H., Wang, Z., Zhou, Y., Zhou, X.H., et al., 2007. Influence of meteorological conditions and particulate matter on visual range impairment in Jinan, China. Sci. Total Environ. 383 (1–3), 164–173.

Yang, F.M., Tan, J.H., Zhao, Q., Du, Z., He, K., Ma, Y.J., et al., 2011. Characteristics of $PM_{2.5}$ speciation in representative megacities and across China. Atmos. Chem. Phys. 11 (11), 5207–5219.

Yu, H., Wu, C., Wu, D., Yu, J.Z., 2010. Size distributions of elemental carbon and its contribution to light extinction in urban and rural locations in the pearl river delta region, China. Atmos. Chem. Phys. 10 (11), 5107–5119.

Zhang, Q., He, K.B., Huo, H., 2012a. Cleaning China's air. Nature 484, 161–162.

Zhang, Y.L., Wang, X.M., Blake, D.R., Li, L.F., Zhang, Z., Wang, S.Y., et al., 2012b. Aromatic hydrocarbons as ozone precursors before and after outbreak of the 2008 financial crisis in the Pearl River Delta region, south China. J. Geophys. Res.-Atmos. 117 (D15), D15306.

Zhang, Y.L., Wang, X.M., Li, G.H., Yang, W.Q., Huang, Z.H., Zhang, Z., et al., 2015. Emission factors of fine particles, carbonaceous aerosols and traces gases from road vehicles: recent tests in an urban tunnel in the Pearl River Delta, China. Atmos. Environ. http://dx.doi.org/10.1016/j.atmosenv.2015.08.024.

Zhao, P.S., Zhang, X.L., Xu, X.F., Zhao, X.J., 2011. Long-term visibility trends and characteristics in the region of Beijing, Tianjin, and Hebei, China. Atmos. Res. 101 (3), 711–718.